Chemical Papers (2019) 73:2845–2855
https://doi.org/10.1007/s11696-019-00836-4

ORIGINAL PAPER

Graphite-on-paper-based resistive sensing device for aqueous chemical identification

Reza Rashidi[1] · Jasem Alenezi[1] · Jennifer Czechowski[1] · Justin Niver[1] · Sulaiman Mohammad[1]

Received: 13 January 2019 / Accepted: 28 May 2019 / Published online: 3 June 2019

Abstract

This article exhibits an innovative, low-cost, and environmentally friendly sensor for identifying aqueous chemicals. The sensor is able to distinguish between different varieties of chemicals including acids, bases, deionized water, and solvents. The sensing device can be used in a wide range of industrial applications that require low-cost, accurate methods of chemical detection. The device can identify different chemicals based on changes in the electrical resistance of graphite which is used as a sensing element. A graphite line was drawn on a sheet of paper using a pencil that was used as the test strip and placed in a custom-made test fixture, providing a controlled environment once the graphite test strip was in contact with electrical contacts mounted in the fixture. The electrical contacts of the fixture were connected to a data acquisition device which measured and recorded voltage outputs using LabVIEW software. The data collected were then used to compute the electrical resistance. The solvent analysed in this research was isopropyl alcohol. The acids analysed were nitric acid, sulphuric acid, hydrochloric acid, and hydrogen peroxide. The base analysed was ammonium hydroxide. Tests were performed by placing two droplets of each chemical onto the paper through an inlet hole located at the top of the test fixture. All tests were performed at a constant temperature. The electrical voltage was recorded every millisecond once the chemical was dropped onto the test strip through the hole in the test fixture. Electrical resistance versus time plots displayed a unique curve for each chemical analysed which may be used for chemical identification.

Keywords Chemical sensing device · Chemical sensor · Instrumentation · Graphite-on-paper · Chemical identification · Chemical detection

Introduction

In the last two decades, microelectromechanical systems have been extensively used in a wide range of applications due to their beneficial features which include high sensitivity, low cost, small size, and rapid response (Amjadi et al. 2016; Blank et al. 2016; Mohammadi et al. 2010, 2011, 2013; Sprager and Juric 2015; Silvera-Tawil et al. 2015; Triantafyllou et al. 2016; Wei and Xu 2015). Within these applications, chemical detection using low-cost sensors and instrumentation has attracted attention in diverse areas such as industrial, medical, environmental, and agricultural industries. There is an increasing demand for the development MEMS devices that have the ability to accurately detect chemicals in either liquid, gas states, or ions (Neri 2015; Barsan et al. 2015; Yu et al. 2005; Mohammadi et al. 2012; Waggoner and Craighead 2007; Jalali Sarvestani and Ahmadi 2018a, b; Jalali Sarvestani et al. 2018; Sharifi et al. 2017). Paper-based sensing devices have also been widely used in applications such as food quality control (Zhang et al. 2014; Badawy and El-Aswad 2014), environmental control (Das et al. 2012; Andersson et al. 2012), and in health-care testing (Kumar et al. 2015; Li et al. 2015). This is due to their flexibility, light weight, low cost, environmental friendliness, and availability (Dungchai et al. 2011; Zhao and van den Berg 2008). Paper-based sensing devices were predominantly utilized for various chemical detection applications (Sarfraz et al. 2013; Cinti et al. 2016; Chen et al. 2016; Hatai et al. 2012; Jiang et al. 2014; Luo et al. 2017).

Within the paper-based sensors, proof of concept of graphite-on-paper sensors has been recently demonstrated.

✉ Reza Rashidi
rashidr@alfredstate.edu

[1] Department of Mechanical and Electrical Engineering Technology, Alfred State College, State University of New York, Alfred, NY 14802, USA

Graphite-on-paper used as a sensing device has shown great potential in the production of disposable, ecologically friendly, inexpensive, small-sized, and flexible sensing devices. These sensors include thermal flow sensors used in human respiratory monitoring (Dinh et al. 2017), moisture sensors for breath monitoring (Güder et al. 2016), piezoresistive force sensors (Ren et al. 2012), ultraviolet photoconductive sensors (Gimenez et al. 2010; ul Hasan et al. 2012), strain sensors used in motion detection for humans (Yamada et al. 2011; Liao et al. 2015), tactile sensors (Phan et al. 2015), temperature sensors (Dinh et al. 2015), and other flexible electronics (Dinh et al. 2016; Zheng et al. 2011). Paper strips used for graphite-on-paper sensing devices are porous which make it possible for the graphite particles to be deposited over a larger area of the paper surface. This would not be possible when using other nonporous materials such as plastic or glass. Graphite has a structure of layered carbon atoms and is a carbon allotrope. The atoms of graphite have three sites that are bonded covalently and one electron that is unrestricted, thus making graphite electrically conductive (Delhaes 2000). When the graphite is drawn on paper using a pencil, graphite particles are deposited into the pores of the paper surface. The graphite-on-paper can then be used as the sensing element in various devices.

This article exhibits that graphite-on-paper devices may function as a liquid chemical sensor that can accurately detect various liquid chemicals which include water, solvents, bases, and acids. The benefits of using graphite-on-paper for the detection of liquid chemicals are that it is inexpensive, biodegradable, and simple to fabricate; however, as a disadvantage, the graphite used in paper sensing devices is also sensitive to vibrations and temperature changes which may influence the sensor reading. Research was recently conducted that showed the proof of concept of a disposable electroanalytical device, which was made by drawing graphite lines on corrugated fibreboard platforms using common pencils for measuring the concentration of monoaromatic catechol hydrocarbons (Orzari et al. 2018). Unlike the device that used corrugated fibreboard platforms, the device presented in this article was developed using regular printing paper which has a different structure. In addition, a paper-based three-electrode electrochemical device fabricated using a digitally controlled plotter/cutter and a mechanical pencil was developed to analyse vitamin B6 in food supplements (Dossi et al. 2017). Unlike the device which used a three-electrode method, the device presented in this article explores potentials for chemical detection using a two-electrode resistive method. Furthermore, a flexible pencil-drawn electrochemical sensor was investigated to electrocatalytically detect nicotinamide adenine dinucleotide. The bare pencil-drawn surface was enhanced using subsequent oxidation and reduction processes, leading to chemical and structural transformations on the electrode surface (Santhiago et al. 2017). Unlike requiring treatment of the original surface, the device presented in this article works using the low-cost graphite lines drawn on an ordinary paper without treatment of the surface.

Experimental

A schematic overview of the test method used in this research is illustrated in Fig. 1. Two major parts of the setup include a test fixture and measurement devices.

A custom test fixture was created to house the graphite test strip which is displayed in Fig. 2. The test fixture was designed with the use of the SolidWorks modelling program and made by means of an Alunar M505 3D printer and 1.75 mm black Pxmalion printing plastic. The test fixture included a 30 mm × 10 mm × 12 mm upper section with a large inlet hole located in its centre that was 6 mm in diameter. The upper section also included two smaller holes that were 2.5 mm in diameter positioned at each end. The holes positioned at the ends of the upper section allowed conductive copper wires to be soldered into those locations which created electrical connections. The test fixture included a lower section with the measurements of 50 mm × 12 mm × 3 mm, which housed the graphite-on-paper test strip, and the upper section of the test fixture was then placed on top of the lower section, which provided a contained area for the test strip. The test fixture also prevented the copper wires from being directly in contact with the chemical being tested.

To uniformly and economically draw the graphite on the paper for consistent experiments, a 80 mm × 6 mm × 6 mm smooth #2 Bic HB graphite bar which contained 68% carbon and 26% clay was used to manually sketch graphite on the entire surface of an A5 75 g/m^2 white sheet of acid-free MagTec paper for about 30 s on an area. The average drawing speed and pressure on the graphite bar was 0.15 m/s and 6 kPa. The surface resistivity was controlled using a four-point probe on various locations of the paper. The paper was then cut into several 40 mm × 6 mm pieces used for different experiments. It was assumed that the surface resistivity would be uniform in all pieces if one can draw the graphite on the paper at the same time. However, if any variation in resistivity was observed among the graphite-on-paper pieces, the results were normalized accordingly. A piece of the processed paper was then placed in the test fixture equipped with electrical contacts. The 3D printed test fixture housing the graphite-on-paper sensing element and the graphite bar along with a piece of cut paper are shown in Fig. 3. The electrical contacts were attached to a data acquisition device (DAQ) along with LabVIEW software to allow for the recording of changes in voltage which was later used to calculate the electrical resistance.

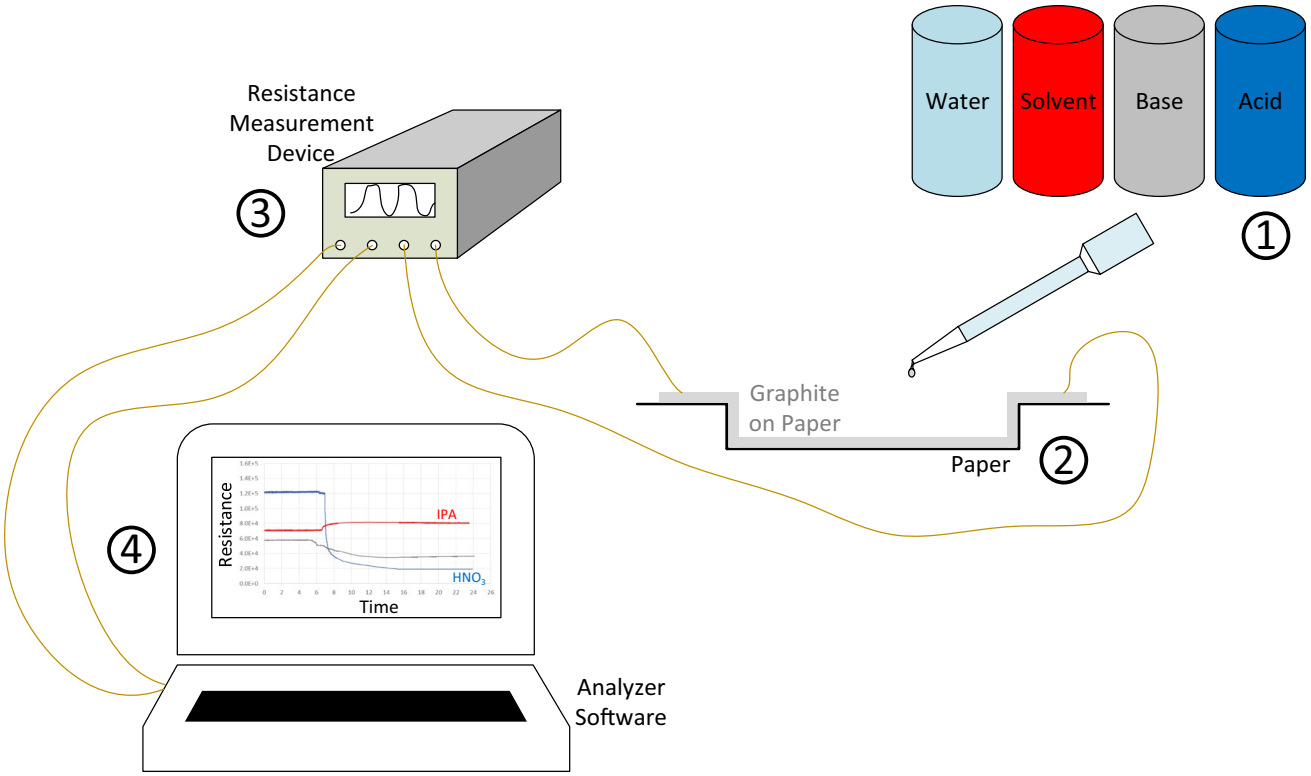

Fig. 1 Schematic overview of the test method used in this research

Fig. 2 Test fixture created to house the graphite-on-paper sensing element

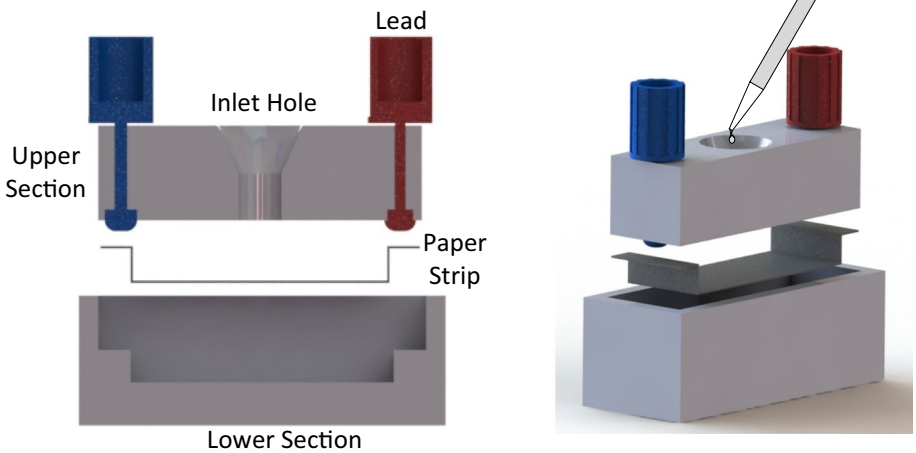

A custom circuit was created to measure and record voltages and compute variations in electrical resistance of the test strip using a USB 6003 multifunctional DAQ produced by National Instruments. Ten volts was delivered to the circuit with a known 3.840 kΩ resistor set up in a series configuration. The DAQ circuit was then connected in series with the contacts of the test fixture as displayed in Fig. 4. The drops in voltage across the graphite-on-paper test strip and the 3.840 kΩ resistor were measured by the DAQ card and logged using LabVIEW software each millisecond. Resistance changes of the test strip caused by the contact of various liquid chemicals were calculated based on the documented voltages using Kirchhoff's law.

The experimental arrangement used in the testing of various types of chemicals at room temperature is displayed in Fig. 5. Two drops of each chemical were

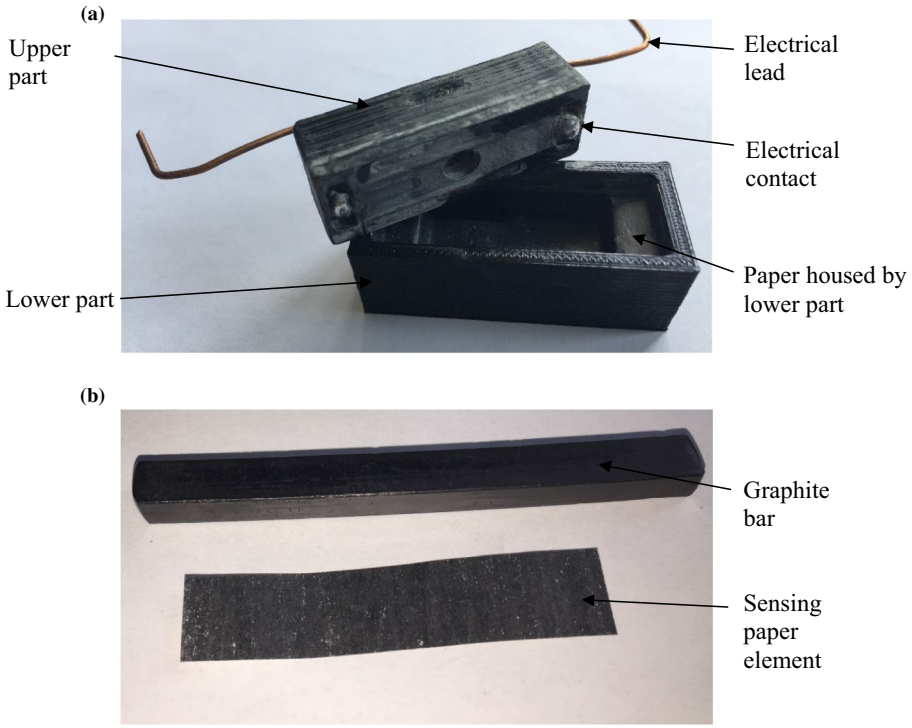

Fig. 3 **a** Fabricated test fixture housing including the 3D printed upper and lower parts housing the graphite-on-paper sensing element. **b** A graphite bar along with a piece of cut paper

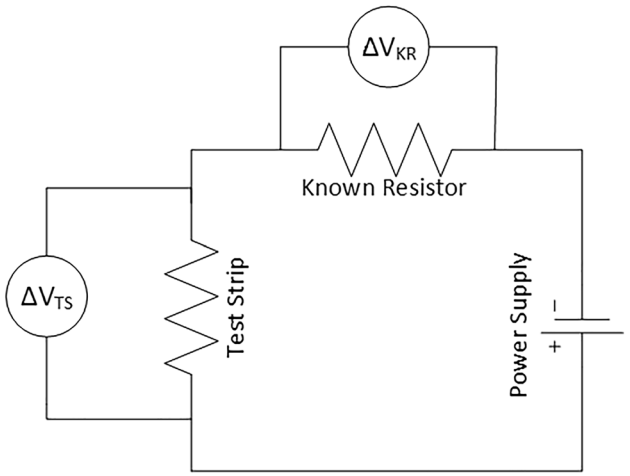

Fig. 4 The circuit used to compute changes in electrical resistance of the test strip using a known resistor

deposited onto the graphite-on-paper test strip through the hole in the centre of the upper section of the test fixture using a disposable pipette. As soon as the liquid chemical was dropped on the paper, the voltage was recorded every millisecond. The test fixture was sanitized and a new test strip was placed in the fixture after every trial.

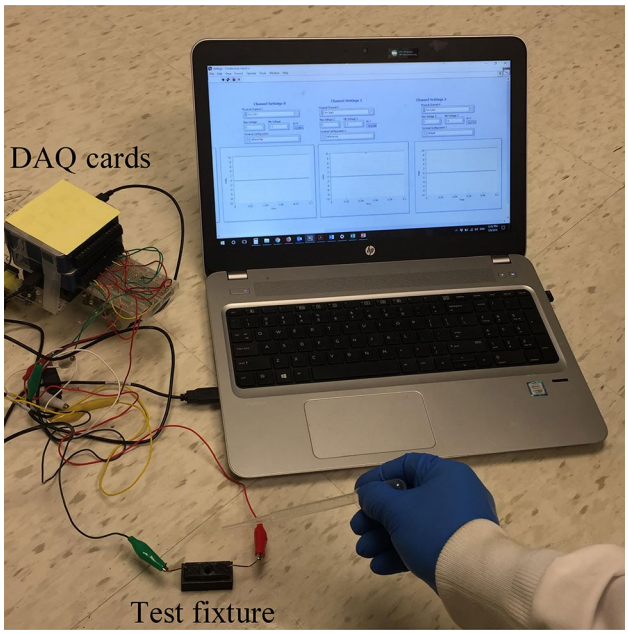

Fig. 5 Arrangement used in the testing of various types of chemicals at room temperature. The setup includes the test fixture connected to the DAQ card to measure and record changes in voltage across the paper strip

Results and discussion

The trials conducted on the available chemicals were grouped into solvents, bases, acids, and deionized water. The resistance versus time curves generated after each trial could be closely duplicated for each chemical. The data collected were analysed in the three different methods. First, the resistance was studied 1–2 s after a change in resistance was witnessed. That change in resistance was then used as a criterion for identification of the chemicals. Second, the final resistance was recorded 10 s after the initial resistance change and was used as the second criterion for identifying the chemicals. Third, the chemical was analysed based on its gradient of resistance over time and was used as the third criterion for detection of the chemical.

The solvent analysed in this research was 99.5% isopropyl alcohol (IPA). The results collected for IPA are displayed in Fig. 6a. The curve generated using the data collected from the IPA trial increased gradually when the graphite-on-paper test strip was exposed to the solvent. In the results collected for the deionized water trial, the curve generated using the data recorded considerably decreased and then levelled off as shown in Fig. 6b.

Furthermore, the acids examined in this research included 70% nitric acid (HNO_3), 96% sulphuric acid (H_2SO_4), 38% hydrochloric acid (HCl), and 30% hydrogen peroxide (H_2O_2). The results of the trials performed on the four acids are displayed in Fig. 6c. All four acids tested exhibited a decrease in the resistance when the test strip was exposed to the acid; however, the curve generated from the data collected during the nitric acid trial significantly dropped compared with the other acids. Additionally, the initial decrease in the curve generated from the hydrochloric acid trial was slightly greater than of the one generated from the sulphuric acid. The resistance in the curve generated from the

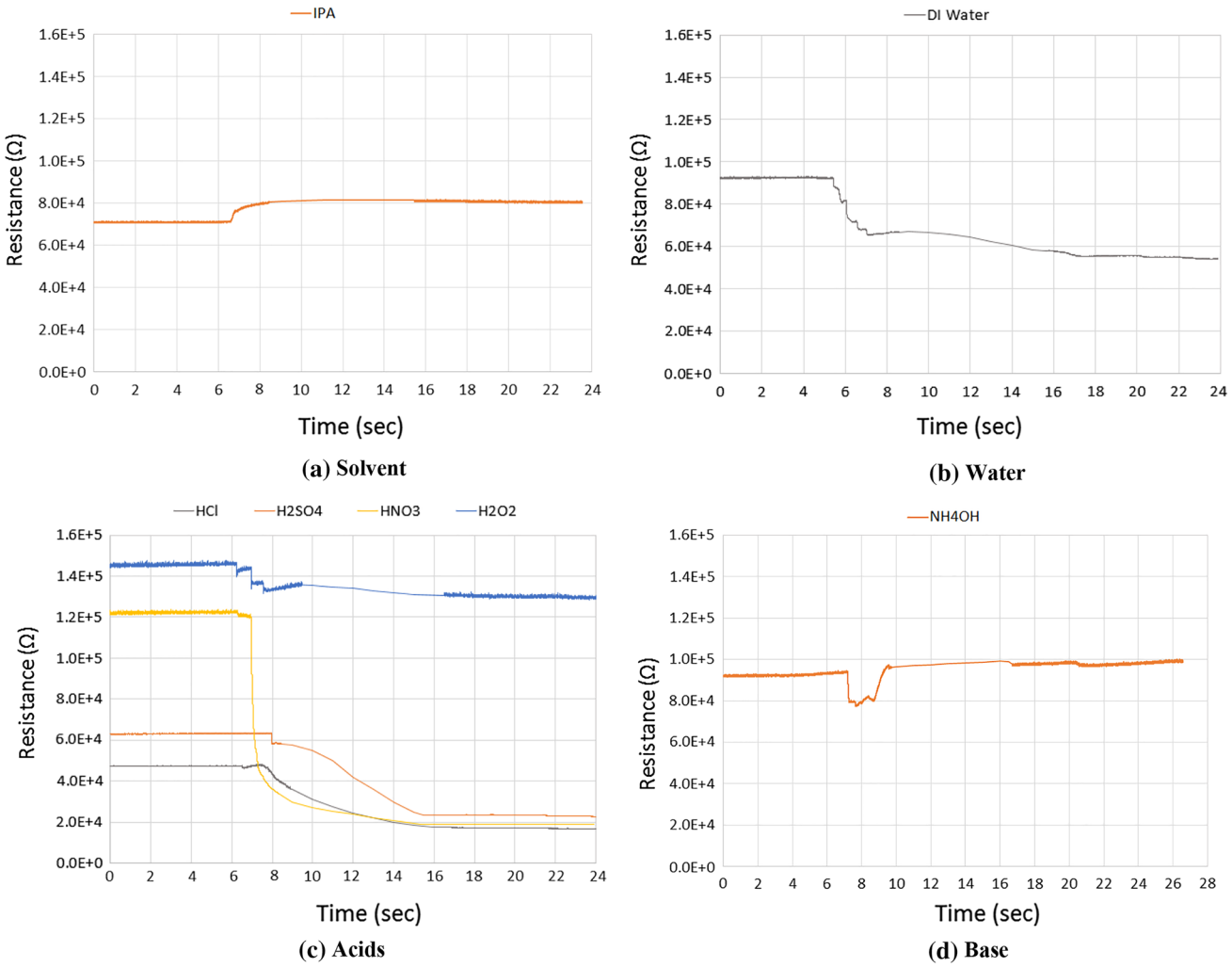

Fig. 6 Resistance versus time curves of graphite-on-paper exposed to solvent (**a**), DI water (**b**), acids (**c**) and base (**d**)

hydrogen peroxide trial slightly decreased and then levelled off. All four curves generated by the acids levelled off after a few seconds.

The base analysed in this experiment was 29% ammonium hydroxide (NH_4OH) and the results are displayed in Fig. 6d. The generated curve showed a sharp initial drop in the resistance followed by a reversion back to almost its original position after a few seconds.

To quantitatively differentiate the chemicals analysed using the second above-mentioned criterion, the final resistance was calculated 10 s after the initial resistance change of the graphite-on-paper test strip. The initial and final resistance changes after 1–2 s and 10 s for each chemical tested are displayed in Fig. 7. Additionally, the percentage change in the resistance after 1–2 s and 10 s is displayed in Fig. 8. The final resistance values are presented in Table 1. Among acids, the lowest drops in resistance occurred during the hydrogen peroxide trial, and the greatest drops in resistance transpired during the nitric acid trial. Furthermore, the IPA displayed a resistance increase. The deionized water indicated a significant drop in the resistance of the graphite-on-paper test strip.

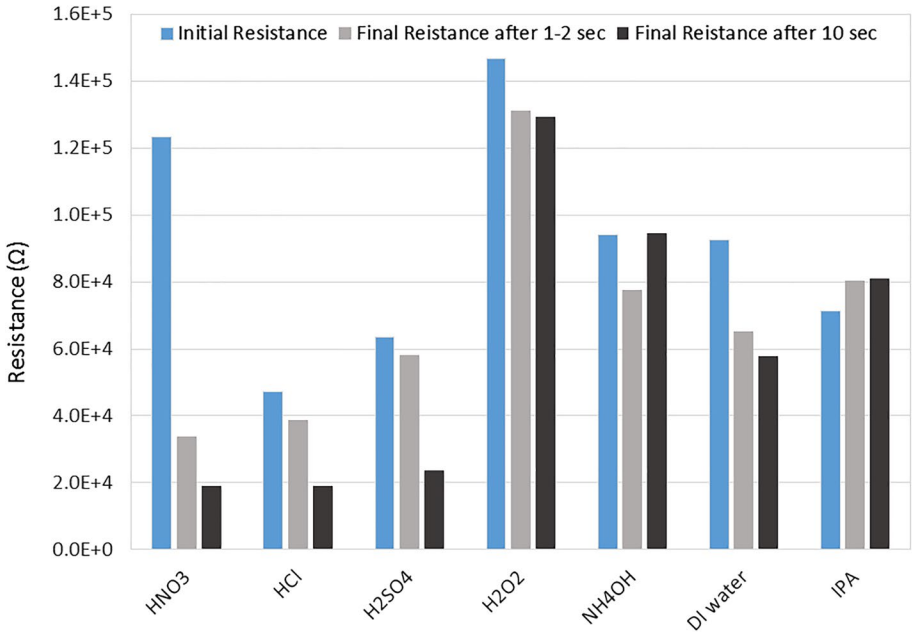

Fig. 7 Resistance of the graphite-on-paper, including readings before the test and 1–2 s and 10 s after exposure to chemicals

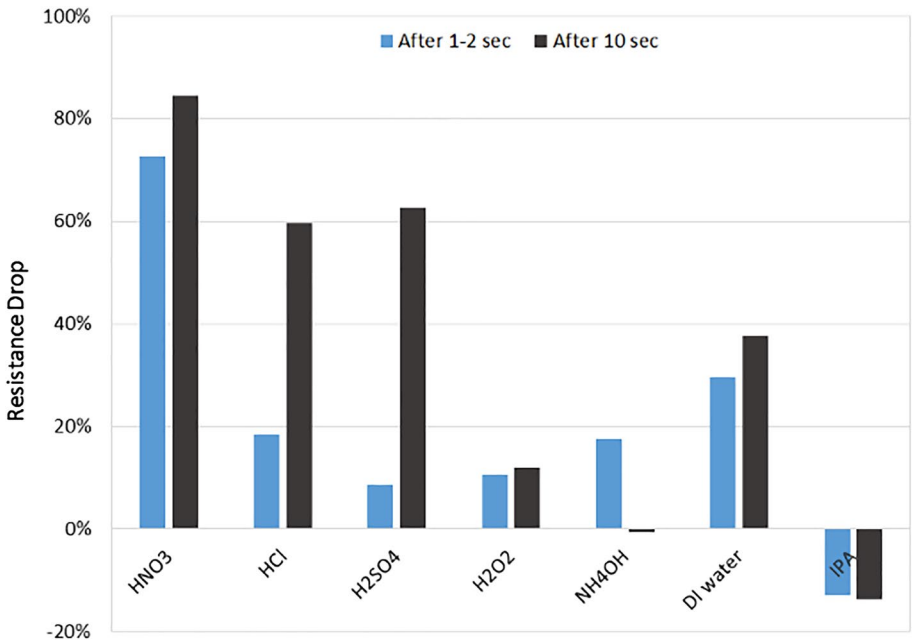

Fig. 8 Change in resistance of the graphite-on-paper, 1–2 s and 10 s after exposure to chemicals

Table 1 Resistance points of the graphite-on-paper exposed to different chemicals and their drop percentage relative to the initial resistance in 1–2 s and 10 s after the initial drop

Chemical	Initial resistance (Ω)	Resistance after 1–2 s (Ω)	Resistance drop after 1–2 s (%)	Final resistance (Ω)	Final resistance drop (%)	Initial resistance gradient (Ω/s)
HNO_3	123,445	33,766	72.6	19,126	84.5	69,990
HCl	47,371	38,677	18.4	19,095	59.7	13,306
H_2SO_4	63,455	58,056	8.5	23,709	62.6	20,064
H_2O_2	146,873	131,272	10.6	129,301	12.0	10,782
NH_4OH	93,961	77,504	17.5	94,507	−0.6	13,707
DI water	92,670	65,181	29.7	57,825	37.6	20,405
IPA	71,133	80,233	−12.8	80,864	−13.7	−4295

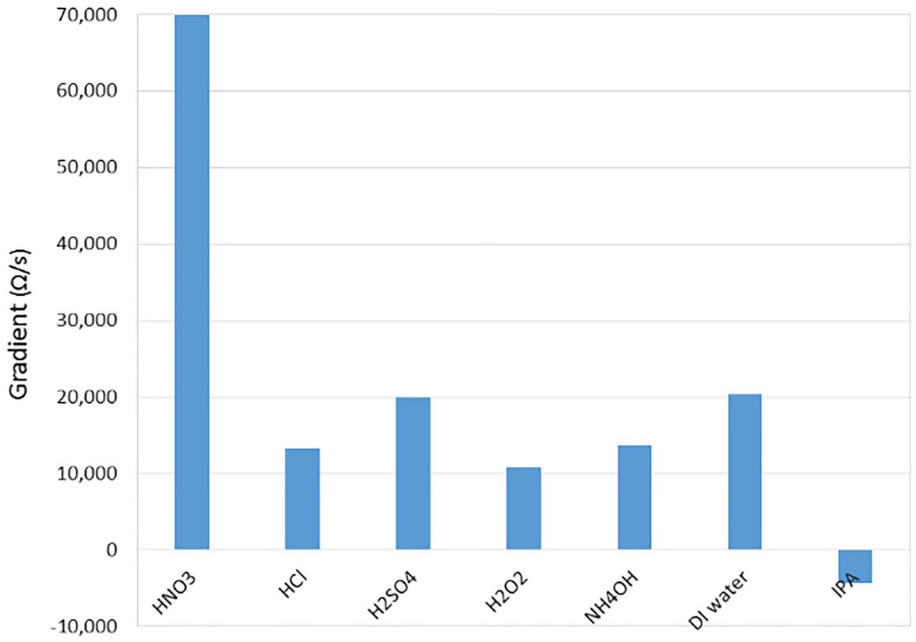

Fig. 9 Gradient of initial resistance change over time after graphite-on-paper exposed to different chemicals

In addition, the initial gradient of resistance over time was determined for each chemical and the results are shown in Fig. 9 and in Table 1. In general, all chemicals showed a drop in resistance; only IPA illustrated an increase in resistance. Acetone showed a gradual drop in resistance, while the IPA had a gradual increase in resistance. The curve for water showed the second highest gradient after nitric acid, even though its gradient was similar to the one for sulphuric acid. In the group of acids, nitric acid was distinguishable with a very high gradient compared with other acids. This distinguished this acid from other acids. The gradient of hydrochloric acid was slightly higher than the one for hydrogen peroxide. In the group of bases, ammonium hydroxide showed a higher gradient compared with the one for TMAH.

To ensure the repeatability in the experiments, the experiments were repeated for nitric acid and the results showed that the percentage in the final resistance drop was repeatable with standard deviations of 1.98%.

The data revealed that the IPA had increasing final resistance produced after 10 s. An explanation for this is that the solvent evaporates rapidly at room temperature. Heat is required for the IPA to evaporate which is taken from the surrounding location (Liao et al. 2015). Consequently, the instantaneous temperature drop is a result of the evaporation of IPA and is responsible for the resistance increase. This resistance increase is due to graphite's negative temperature coefficient of resistance (Dinh et al. 2017) and is displayed in the data collected for this article. The results obtained in this experiment indicate that the resistance is directly affected by temperature.

Paper has a hygroscopic character which means it has a tendency to adsorb water from the surrounding environment. Therefore, upon exposure to water, the ionic conductivity of the paper increases proportionally to the amount of water on the surface of the cellulose fibres (Güder et al. 2016; Mark and Borch 2001; Tobjörk and Österbacka 2011). This likely

Table 2 Electrical conductivity of the chemicals used in the experiments, computed or extracted from references (Weast 1989; Wolf 1966)

Chemical	Concentration (wt%)	Electrical conductivity (mS/cm)
HNO_3	70	415.4
H_2SO_4	96	37.5
HCl	38	732
H_2O_2	30	4.50E−03
IPA	99.5	6.00E−05
NH_4OH	29	0.75
HB graphite	68	5.4E04

caused a drop in resistance of the graphite-on-paper. In addition, unlike IPA, water makes strong intermolecular bonds and therefore evaporates slowly.

The paper acts as a substrate to hold the graphite on it. As the paper is an insulator compared with graphite, the current mainly passes through the graphite before exposure to chemicals. When exposed, the chemical absorbed by the paper substrate causes the paper to transmit a part of the current through paper, reducing the resistance. The paper in this case acts as a chemical holder and its quality may not have a significant effect on the results. Similar papers were used in all trials and therefore the quality and type of paper were consistent in all experiments.

All four acids analysed in this experiment displayed an initial resistance drop; however, acids are electrolytes and contain dissolved hydrogen cations (H^+) which conduct electricity because they carry electrical charges. Consequently, the resistance of the graphite on the test strip would drop after exposure to an acid. Strong acids including hydrochloric acid, sulphuric acid, and nitric acid dissociate entirely and generate additional H^+ cations. Thus, this is likely the cause of the substantial final resistance drop. On the other hand, their contribution in electrical conductivity depends on their concentration as presented in Table 2. Hydrogen peroxide is a weak acid and contributes less in increasing the conductivity due to generating fewer H^+ cations and, therefore, causes less drop in resistance of the graphite-on-paper as displayed in Table 2.

Ammonium hydroxide is a basic electrolyte that consists of dissolved hydroxide anions (OH^-) which conduct electricity and act as charge carriers. NH_4OH which is a weak base dissociates slightly in water and that is the reason for the drop in resistance of graphite. The curve associated with NH_4OH dropped and then had a sharp increase which might be due to a chemical reaction between the paper and the chemical. Comparing the acids and bases, the molar conductivity of H^+ cations (0.34982 S L/mol cm) produced by acids in water is 1.75 times that of OH^- anions (0.1986 S L/mol cm) produced by bases in water. This likely caused a less of a contribution of the bases in dropping the resistance of the graphite-on-paper compared with acids.

The microstructure of specimens were photographed before the test and immediately after chemical exposure in wet condition at 50× and 200× magnifications using an optical microscope. Figure 10 shows the microstructure images for all seven chemicals. In all specimens the graphite appeared to remain intact. In addition, the paper substrates were not degraded by the chemicals and it kept its integrity similar to the condition before exposure.

Even though the current device is a handheld one, there is still room for further miniaturization as a direction for future work. To further scale the device down, one of the methods is to deposit amorphous carbon thin films on a paper using evaporation or sputtering techniques. A polyimide film pattered by a laser beam can be used as a physical mask for the deposition to define conductive paper elements. The housing of the device can be still 3D printed with a smaller size, but the features would be in microscale. One of the advantages of this method is the ability for batch fabrication.

Conclusions

This article examined the use of graphite-on-paper as a sensing element in a device to identify various aqueous chemicals. A specialized test fixture prepared with a graphite-on-paper test strip consistently distinguished between various liquid chemicals after dropping a specific amount of each chemical onto a test strip through an inlet hole in the test fixture. There was no contact between the sensor leads and chemicals, and the only area exposed to the chemicals was the graphite-on-paper test strip. The solvent detection principle was based on changes in temperature of thermosensitive graphite due to chemical evaporation at room temperature. The stronger the base or acid, the greater is the conductivity and the lesser is the resistivity. Resistance of the graphite-on-paper displayed dissimilar behaviour after exposure to various liquid chemicals. The amount of ions dissolved in each liquid chemical placed in contact with the graphite-on-paper had an impact on the resistivity generated. This low-cost chemical identification device may be used in multiple industries where the testing of chemicals is essential.

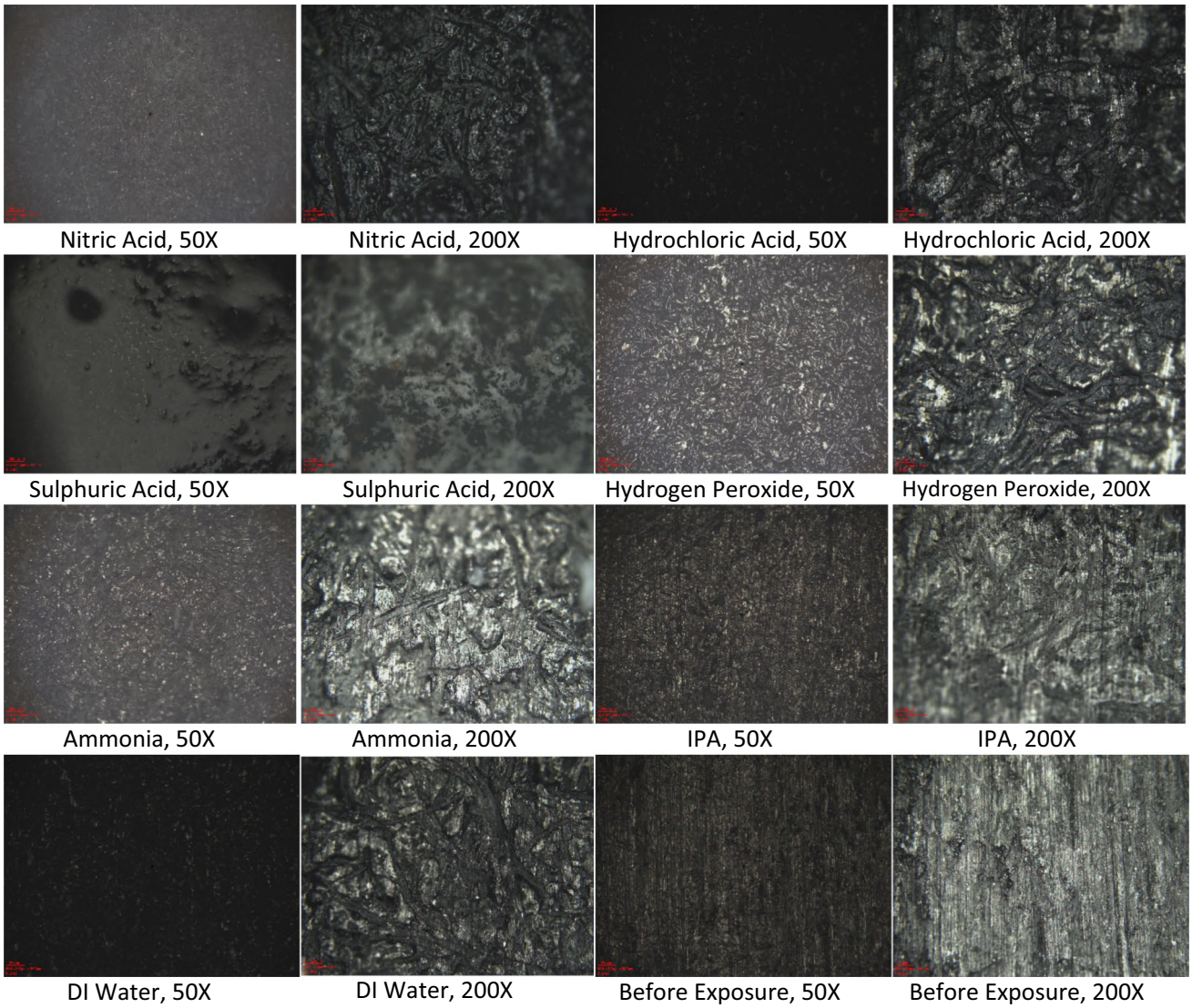

Fig. 10 The microstructure of specimens before and after (in wet condition) exposure at ×50 and ×200 magnifications

Compliance with ethical standards

Conflict of interest On behalf of all authors, the corresponding author states that there is no conflict of interest.

References

Amjadi M, Kyung KU, Park I, Sitti M (2016) Stretchable, skin-mountable, and wearable strain sensors and their potential applications: a review. Adv Funct Mater 26(11):1678–1698

Andersson H, Manuilskiy A, Unander T, Lidenmark C, Forsberg S, Nilsson HE (2012) Inkjet printed silver nanoparticle humidity sensor with memory effect on paper. IEEE Sens J 12(6):1901–1905

Badawy ME, El-Aswad AF (2014) Bioactive paper sensor based on the acetylcholinesterase for the rapid detection of organophosphate and carbamate pesticides. Int J Anal Chem 2014:536823. https://doi.org/10.1155/2014/536823

Barsan MM, Ghica ME, Brett CM (2015) Electrochemical sensors and biosensors based on redox polymer/carbon nanotube modified electrodes: a review. Anal Chim Acta 30(881):1–23

Blank TA, Eksperiandova LP, Belikov KN (2016) Recent trends of ceramic humidity sensors development: a review. Sens Actuators B Chem 2(228):416–442

Chen X, Yu S, Yang L, Wang J, Jiang C (2016) Fluorescence and visual detection of fluoride ions using a photoluminescent graphene oxide paper sensor. Nanoscale 8(28):13669–13677

Cinti S, Talarico D, Palleschi G, Moscone D, Arduini F (2016) Novel reagentless paper-based screen-printed electrochemical sensor to detect phosphate. Anal Chim Acta 5(919):78–84

Das P, Ghosh A, Bhatt H, Das A (2012) A highly selective and dual responsive test paper sensor of Hg^{2+}/Cr^{3+} for naked eye detection in neutral water. RSC Adv 2(9):3714–3721

Delhaes P (2000) Graphite and precursors. CRC Press, Boca Raton

Dinh T, Phan H, Dao DV, Woodfield P, Qamar A, Nguyen N (2015) Graphite on paper as material for sensitive thermoresistive sensors. J Mater Chem C 3(34):8776–8779

Dinh T, Phan HP, Qamar A, Nguyen NT, Dao DV (2016) Flexible and multifunctional electronics fabricated by a solvent-free and user-friendly method RSC. Advances 6(81):77267–77274

Dinh T, Phan HP, Qamar A, Nguyen TK, Woodfield P, Zhu Y, Nguyen NT, Dao DV (2017) Environment-friendly wearable thermal flow sensors for noninvasive respiratory monitoring. In: IEEE 30th international conference on micro electro mechanical systems (MEMS), pp 993–996

Dossi N, Petrazzi S, Toniolo R, Tubaro F, Terzi F, Piccin E, Svigelj R, Bontempelli G (2017) Digitally controlled procedure for assembling fully drawn paper-based electroanalytical platforms. Anal Chem 89(19):10454–10460

Dungchai W, Chailapakul O, Henry CS (2011) A low-cost, simple, and rapid fabrication method for paper-based microfluidics using wax screen-printing. Analyst 136(1):77–82

Gimenez AJ, Yanez-Limon JM, Seminario JM (2010) ZnO-paper based photoconductive UV sensor. J Phys Chem C 115(1):282–287

Güder F, Ainla A, Redston J, Mosadegh B, Glavan A, Martin TJ, Whitesides GM (2016) Paper-based electrical respiration sensor. Angew Chem Int Ed 55(19):5727–5732

Hatai J, Pal S, Jose GP, Bandyopadhyay S (2012) Histidine based fluorescence sensor detects Hg^{2+} in solution, paper strips, and in cells. Inorg Chem 51(19):10129–10135

Jalali Sarvestani MR, Ahmadi R (2018a) Evaluating the performance of 2,3-dihydro-1*H*-phenothiazine-4(5a*H*)-one as an ionophore in construction of a cation selective electrode by density functional theory. Int J New Chem 1:409–418

Jalali Sarvestani MR, Ahmadi R (2018b) Determination of Mn^{2+} in pharmaceutical supplements by a novel coated graphite electrode based on zolpidem as a neutral ion carrier. Anal Bioanal Chem Res 5(2):273–284

Jalali Sarvestani MR, Hajiaghababaei L, Najafpour J, Suzangarzadeh S (2018) 1-(6-Choloroquinoxaline-2-yl)hydrazine as an excellent ionophore for preparation of a cobalt selective electrode and potentiometric measuring of vitamin B-12 in pharmaceutical samples. Anal Bioanal Electrochem 10(6):675–698

Jiang Z, Li J, Aslan H, Li Q, Li Y, Chen M, Huang Y, Froning JP, Otyepka M, Zbořil R, Besenbacher F (2014) A high efficiency H_2S gas sensor material: paper like Fe_2O_3/graphene nanosheets and structural alignment dependency of device efficiency. J Mater Chem A 2(19):6714–6717

Kumar S, Willander M, Sharma JG, Malhotra BD (2015) A solution processed carbon nanotube modified conducting paper sensor for cancer detection. J Mater Chem B. 3(48):9305–9314

Li CG, Joung HA, Noh H, Song MB, Kim MG, Jung H (2015) One-touch-activated blood multidiagnostic system using a minimally invasive hollow microneedle integrated with a paper-based sensor. Lab Chip 15(16):3286–3292

Liao X, Liao Q, Yan X, Liang Q, Si H, Li M, Wu H, Cao S, Zhang Y (2015) Flexible and highly sensitive strain sensors fabricated by pencil drawn for wearable monitor. Adv Funct Mater 25(16):2395–2401

Luo X, You K, Hu Y, Yang S, Pan X, Wang Z, Chen W, Gu H (2017) Rapid hydrogen sensing response and aging of α-MoO_3 nanowires paper sensor. Int J Hydrog Energy 42(12):8399–8405

Mark RE, Borch J (2001) Handbook of physical testing of paper, vol 1. CRC Press, Boca Raton

Mohammadi AR, Graham TC, Bennington CP, Chiao M (2010) Development of a compensated capacitive pressure and temperature sensor using adhesive bonding and chemical-resistant coating for multiphase chemical reactors. Sens Actuators A Phys 163(2):471–480

Mohammadi AR, Chen K, Ali MS, Takahata K (2011) Radio aneurysm coils for noninvasive detection of cerebral embolization failures: a preliminary study. Biosens Bioelectron 30(1):300–305

Mohammadi AR, Graham TC, Madden JD, Bennington CP (2012) Toward a flow following ionic conductivity and temperature sensor package. Ind Eng Chem Res 51(6):2738–2746

Mohammadi AR, Ali MS, Lappin D, Schlosser C, Takahata K (2013) Inductive antenna stent: design, fabrication and characterization. J Micromech Microeng 23(2):025015

Neri G (2015) First fifty years of chemoresistive gas sensors. Chemosensors 3(1):1–20

Orzari LO, de Araujo Andreotti IA, Bergamini MF, Junior LH, Janegitz BC (2018) Disposable electrode obtained by pencil drawing on corrugated fiberboard substrate. Sens Actuators B Chem 264:20–26

Phan H, Dao DV, Dinh T, Brooke H, Qamar A, Nguyen N, Zhu Y (2015) Graphite-on-paper based tactile sensors using plastic laminating technique. In: 28th IEEE international conference on micro electro mechanical systems (MEMS), pp 825–828

Ren TL, Tian H, Xie D, Yang Y (2012) Flexible graphite-on-paper piezoresistive sensors. Sensors 12(5):6685–6694

Santhiago M, Strauss M, Pereira MP, Chagas AS, Bufon CC (2017) Direct drawing method of graphite onto paper for high-performance flexible electrochemical sensors. ACS Appl Mater Interfaces 9(13):11959–11966

Sarfraz J, Ihalainen P, Määttänen A, Peltonen J, Lindén M (2013) Printed hydrogen sulfide gas sensor on paper substrate based on polyaniline composite. Thin Solid Films 534:621–628

Sharifi A, Hajiaghababaei L, Suzangarzadeh S, Sarvestani MR (2017) Synthesis of 3-((6-methyl-5-oxo-3-thioxo-2,5-dihydro1,2,4-triazin-4(3*H*)-yl)imino)indolin-2-one as an excellent ionophore to the construction of a potentiometric membrane sensor for rapid determination of zinc. Anal Bioanal Electrochem 9(7):888–903

Silvera-Tawil D, Rye D, Velonaki M (2015) Artificial skin and tactile sensing for socially interactive robots: a review. Robot Auton Syst 1(63):230–243

Sprager S, Juric MB (2015) Inertial sensor-based gait recognition: a review. Sensors 15(9):22089–22127

Tobjörk D, Österbacka R (2011) Paper electronics. Adv Mater 23(17):1935–1961

Triantafyllou MS, Weymouth GD, Miao J (2016) Biomimetic survival hydrodynamics and flow sensing. Annu Rev Fluid Mech 3(48):1–24

ul Hasan K, Nur O, Willander M (2012) Screen printed ZnO ultraviolet photoconductive sensor on pencil drawn circuitry over paper. Appl Phys Lett 100(21):211104

Waggoner PS, Craighead HG (2007) Micro-and nanomechanical sensors for environmental, chemical, and biological detection. Lab Chip 7(10):1238–1255

Weast RC (1989) CRC handbook of chemistry, and physics, 70th edn. CRC Press, Boca Raton, p D-221

Wei Y, Xu Q (2015) An overview of micro-force sensing techniques. Sens Actuators A 1(234):359–374

Wolf AV (1966) Aqueous solutions and body fluids. Harper and Row, New York

Yamada T, Hayamizu Y, Yamamoto Y, Yomogida Y, Izadi-Najafabadi A, Futaba DN, Hata K (2011) A stretchable carbon nanotube strain sensor for human-motion detection. Nat Nanotechnol 6(5):296–301

Yu Q, Chen S, Taylor AD, Homola J, Hock B, Jiang S (2005) Detection of low-molecular-weight domoic acid using surface plasmon resonance sensor. Sens Actuators B Chem 107(1):193–201

Zhang Y, Li H, Niu LY, Yang QZ, Guan YF, Feng L (2014) An SPE-assisted BODIPY fluorometric paper sensor for the highly selective and sensitive determination of Cd^{2+} in complex sample: rice. Analyst 139(12):3146–3153

Zhao W, van den Berg A (2008) Lab on paper. Lab Chip 8(12):1988–1991
Zheng G, Hu L, Wu H, Xie X, Cui Y (2011) Paper supercapacitors by a solvent-free drawing method. Energy Environ Sci 4(9):3368–3373